



Contents List available at VOLKSON PRESS

## New Materials and Intelligent Manufacturing (NMIM)

DOI : <http://doi.org/10.26480/icnmim.01.2018.270.272>Journal Homepage : <https://topicsonchemeng.org/my/>

ISBN: 978-1-948012-12-6



# STUDY ON CATALYTIC ROLES OF TUNGSTEN CARBIDE NANOSPHERES FOR CH<sub>4</sub>/CO<sub>2</sub> REFORMING OVER NI BASED CATALYSTS

Niu Liang, Jin Xing\*

College of chemistry and pharmaceutical engineering, Jilin Institute of Chemical Technology No.45 chengde street, Jilin City, China, 132022  
\*Corresponding Author Email: [jinxing70@163.com](mailto:jinxing70@163.com)

This is an open access article distributed under the Creative Commons Attribution License, which permits unrestricted use, distribution, and reproduction in any medium, provided the original work is properly cited

### ARTICLE DETAILS

### ABSTRACT

#### Article History:

Received 26 June 2018

Accepted 2 July 2018

Available online 1 August 2018

In this paper, WO<sub>3</sub> nanospheres are used carriers and Ni-WC<sub>x</sub> nanospheres are synthesized via the method of incipient impregnation and temperature programming carbonization with the content of Ni is 10%. The presence of Ni promotes the cracking of CH<sub>4</sub>, while the activation of CO<sub>2</sub> takes place on WC<sub>x</sub>. Thus, the deactivation due to carbon accumulation or WC<sub>x</sub> oxidation could be avoided.

#### KEYWORDS

Tungsten carbide nanospheres, Nickel, Methane, Carbon dioxide, Reforming.

## 1. INTRODUCTION

Dry reforming of methane with CO<sub>2</sub> (DRM) has become an interesting alternative for syngas production due to the fact that the greenhouse gases CO<sub>2</sub> and CH<sub>4</sub> can be utilized through the reaction [1,2]. At the same time, The DRM process produces syngas with a H<sub>2</sub>/CO ratio of 1 that is suitable for Fischer-Tropsch (F-T) and carbonyl synthesis the process is a strong endothermic reaction, with a large reaction heat in the generated syngas, which can release stored energy by reversible reaction, and has multiple research values such as science and environmental protection [3]. Both noble and non-noble metals were found to show catalytic activity towards the reaction. But noble metal catalysts are expensive and non-noble metal catalysts (mainly nickel-based catalysts) have the problem of catalyst deactivation due to coking [4,5].

Transition metal carbides have attracted extensive attention over the recent years because their catalytic performances are similar to those of noble metals in reactions [6, 7]. This paper reports the WO<sub>3</sub> nanospheres as the carrier, using the method of volumetric impregnation with the load of Ni was 10% [8, 9]. Then Ni-WC<sub>x</sub> nanospheres bifunctional catalysts are prepared through a series of temperature-programmed processes [10].

## 2. EXPERIMENTAL

### 2.1 Catalyst preparation

We prepared WO<sub>3</sub> nanospheres by stirring an aqueous solution of the pure sodium tungstate and citric acid for 0.5h. Then hydrochloric acid was added to it stirring for 10 min. The above mixture was then transferred into a Teflon-lined stainless-steel autoclave for hydrothermal treatment at 120°C for 24 h. As the autoclave cooled to room temperature naturally, the precipitates were separated by centrifugation, washed with distilled water and absolute ethanol three times, dried at 60°C overnight and calcined at 600°C for 4 h. The nickel nitrate solution was impregnated to the carrier of WO<sub>3</sub> nanospheres. Ni-WC<sub>x</sub> nanospheres were prepared in CH<sub>4</sub>/H<sub>2</sub> (20 vol.% CH<sub>4</sub>) following a series of temperature-programmed processes: temperature was raised from room temperature (RT) to 300 °C at a rate of 5 °C min<sup>-1</sup>, then from 300 to 700 °C at a rate of 1 °C min<sup>-1</sup>, and subsequently kept at 700 °C for 2 h. The above material was cooled down to RT in flowing CH<sub>4</sub>/H<sub>2</sub> and passivated in flowing 1% O<sub>2</sub>/Ar for 12 h.

### 2.2 Catalyst characterization

X-ray powder diffraction (XRD) analysis was conducted using an XRD-6000 (Shimadzu) equipment with Cu Kα radiation (λ = 0.1542 nm), operating at 40kV and 30 mA. BET surface area determinations were performed on a JW-BK-112 (Beijing JWGB Sci. & Tech. Co., Ltd.). Carbon dioxide temperature-programmed oxidation (CO<sub>2</sub>-TPO) studies were performed using a mass spectrometer (OmniStar™ Pfeiffer Vacuum, Germany). With the sample (0.1 g) placed in a quartz tubular reactor, CO<sub>2</sub>-TPO was performed by introducing 10% CO<sub>2</sub>/Ar into the system while the sample temperature was raised from RT to a specific temperature. The signal intensities of CO (m/e = 28) and CO<sub>2</sub> (m/e = 44) were detected. Methane temperature-programmed surface reduction (CH<sub>4</sub>-TPSR) studies were performed using a mass spectrometer. With the sample placed in a quartz tubular reactor, CH<sub>4</sub>-TPSR was carried out by introducing 10% CH<sub>4</sub>/Ar into the system while the sample temperature was raised from RT to a specific temperature. The signal intensities of CH<sub>4</sub> (m/z = 15), H<sub>2</sub> (m/z = 2), H<sub>2</sub>O (m/z = 18), CO (m/z = 28), and CO<sub>2</sub> (m/z = 44) were detected.

### 2.3 Activity measurements

Catalytic tests were performed in a fixed-bed micro-reactor at atmospheric pressure. Before the reaction, the catalyst was activated with a hydrogen flow at 500°C for 1h. Then, the CH<sub>4</sub> and CO<sub>2</sub> (CH<sub>4</sub>/CO<sub>2</sub>=1:1) were introduced into the catalyst bed at a flow rate of 30 mL/min (F/W = 18,000 mL/g h).

## 3. RESULTS

### 3.1 BET

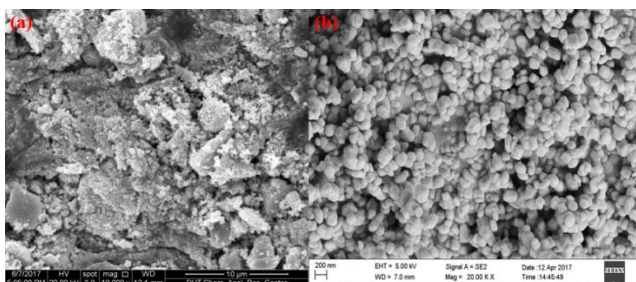
BET analysis on WO<sub>3</sub> and Ni-WC<sub>x</sub> nanospheres was shown in Table 1. Compared with the WO<sub>3</sub> (15 m<sup>2</sup>/g), the surface area of Ni-WC<sub>x</sub> nanospheres was slightly larger and was 63 m<sup>2</sup>/g. Ni supported on the WO<sub>3</sub> and Ni-WC<sub>x</sub> nanospheres, the surface area showed Ni-WC<sub>x</sub> nanospheres can better disperse metal nickel.

**Table 1:** The BET surface analysis data

Sample	$S_{BET}/(m^2.g^{-1})$
WO <sub>3</sub>	15
WO <sub>3</sub> nanospheres	63

**3.2 SEM**

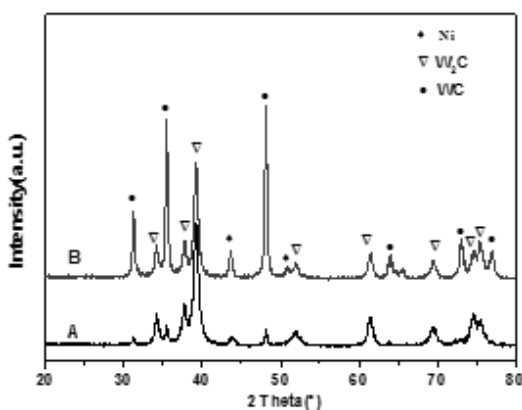
Figure 1 (a) and (b) shows the SEM images of WO<sub>3</sub> and WO<sub>3</sub> nanospheres catalysts. It can be seen that WO<sub>3</sub> nanospheres have a higher specific surface area because of its spherical shape. When Ni is loaded on WO<sub>3</sub> nanospheres, it can better disperse the active metal Ni, promote the cracking of methane and improve the activity of catalyst, which is consistent with the BET characterization results and the activity evaluation results.



**Figure 1:** SEM images of the (a) WO<sub>3</sub> and (b) WO<sub>3</sub> nanospheres catalysts

**3.3 XRD**

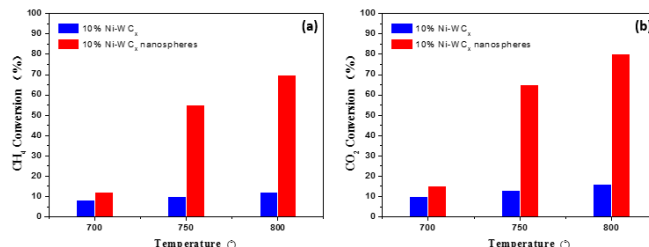
Figure 2 shows the XRD patterns of Ni-WC<sub>x</sub> and Ni-WC<sub>x</sub> nanospheres. The diffraction peaks at 31.5°, 35.7°, 48.3°, 64.1°, 65.8°, 73.2°, 75.6°, 77.1° can be assigned to WC, while those at 34.5°, 38.1°, 39.6°, 52.4°, 61.9°, 69.8°, 75.1°, 76.1° assigned to W<sub>2</sub>C. The diffraction peaks at 44.4° and 51.8° can be assigned to metallic Ni. As calculated by the Scherrer equation based on the metallic Ni diffraction peak at 44.4°, the average particle size of - metallic Ni is 27 and 18.5 nm for Ni-WC<sub>x</sub> and Ni-WC<sub>x</sub> nanospheres, respectively, indicating better dispersion of metallic Ni on the latter. Compared with the Ni-WC<sub>x</sub>, the peaks of Ni-WC<sub>x</sub> nanospheres become much stronger. It is clear that Ni-WC<sub>x</sub> nanospheres catalyst have a good crystal structure.



**Figure 2:** XRD patterns of (A) Ni-WC<sub>x</sub> and (B) Ni-WC<sub>x</sub> nanospheres

**3.4 Activity measure**

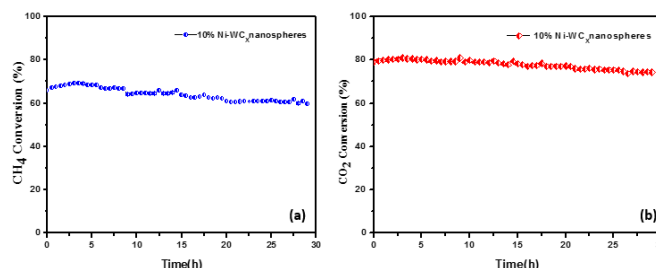
The effects of reaction temperature on catalytic activity of Ni-WC<sub>x</sub> and Ni-WC<sub>x</sub> nanospheres were compared and the results are showed in Figure 3. Over the two catalysts, CH<sub>4</sub> conversion increases with the rise of temperature. The conversions are lowest at 700°C. With increasing temperature to 750°C and 800°C, CH<sub>4</sub> conversions are about 55% and 70% over Ni-WC<sub>x</sub> nanospheres, which are both much higher than that over Ni-WC<sub>x</sub>. We attribute this to the well dispersion of Ni on WO<sub>3</sub> nanospheres that results in promoting the cracking of methane.



**Figure 3:** Effects of reaction temperature on (a) CH<sub>4</sub> conversion and (b) CO<sub>2</sub> conversion over Ni-WC<sub>x</sub> and Ni-WC<sub>x</sub> nanospheres catalysts (atmospheric pressure, F/W = 18000 mL/g h).

**3.5 Stability measurement**

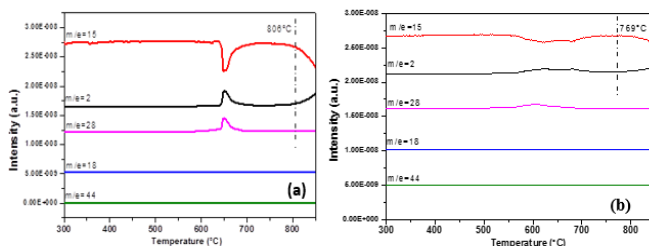
A stability test was carried out at 800°C for 29 h and the results are displayed in Figure 4. The conversions of CH<sub>4</sub> and CO<sub>2</sub> over Ni-WC<sub>x</sub> nanospheres stay at ca.68% and 80%. On the other hand, the conversions of CH<sub>4</sub> and CO<sub>2</sub> over Ni-WC<sub>x</sub> nanospheres remain rather stable across the period of 29 h under the conditions of CH<sub>4</sub>/CO<sub>2</sub>= 1 and WHSV =18000 mL/g h.



**Figure 4:** Catalytic performance over Ni-WC<sub>x</sub> nanospheres catalyst: (a) Conversions of CH<sub>4</sub> and (b) conversions of CO<sub>2</sub> (F/W = 18000 mL/g h, 800 °C, atmospheric pressure)

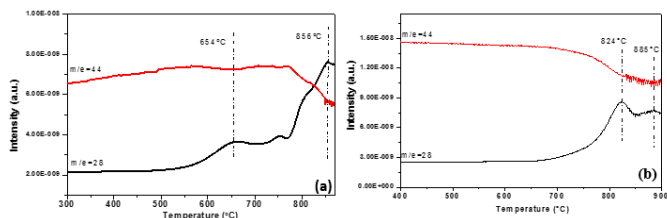
**3.6 Surface reactions of CO<sub>2</sub> and CH<sub>4</sub> over Ni-WC<sub>x</sub> and Ni-WC<sub>x</sub> nanospheres**

Figure 5 displays the results of CH<sub>4</sub>-TPSR over the Ni-WC<sub>x</sub> and Ni-WC<sub>x</sub> nanospheres catalysts obtained in a gas stream of 10% CH<sub>4</sub>/Ar. The consumption peaks of CH<sub>4</sub> at lower temperatures accompanied with the formation of H<sub>2</sub>O, CO and CO<sub>2</sub> is a result of CH<sub>4</sub> interaction with the oxygen species that are formed during passivation [14]. The consumption of CH<sub>4</sub> at higher temperatures accompanied by obvious H<sub>2</sub> formation is ascribed to CH<sub>4</sub> dissociation on the catalysts. In the case of Ni-WC<sub>x</sub>, CH<sub>4</sub> dissociation reaches maximum at 800 °C while over Ni-WC<sub>x</sub> nanospheres, CH<sub>4</sub> dissociation reaches maximum at 769 °C. It is clear that CH<sub>4</sub> dissociation over Ni-WC<sub>x</sub> nanospheres are easier to more significant than that over Ni-WC<sub>x</sub>.



**Figure 5:** CH<sub>4</sub>-TPSR profiles of (a) Ni-WC<sub>x</sub> and (b) Ni-WC<sub>x</sub> nanospheres catalysts

Figure 6 displays the results of CO<sub>2</sub>-TPO studies. In the case of Ni-WC<sub>x</sub>, two peaks are observed, one at 650°C and the other at 840°C. In our previous studies, the former CO<sub>2</sub> consumption peak should be due to the oxidation of surface carbon while the latter to the bulk oxidation of WC<sub>x</sub>. By contrast, the temperature for bulk oxidation of Ni - WC<sub>x</sub> nanospheres is higher than that of Ni-WC<sub>x</sub>. It shows that Ni - WC<sub>x</sub> nanospheres catalyst have better oxidation resistance. It has to do with the results of CH<sub>4</sub>-TPSR characterization the stability test.



**Figure 6:** CO<sub>2</sub>-TPO profiles of (a) Ni-WC<sub>x</sub> and (b) Ni-WC<sub>x</sub> nanospheres catalysts

#### 4. CONCLUSION

It is clear that WO<sub>3</sub> nanospheres has a higher specific surface area and can disperse metal Ni well. At the same time, it also can provide more reactive sites. After temperature programming carbonization, there is a strong interaction between metal Ni and tungsten carbide. The dissociation of CH<sub>4</sub> is catalyzed by Ni, while the activation of CO<sub>2</sub> takes place on the WC<sub>x</sub> nanospheres, which renders Ni-WC<sub>x</sub> nanospheres catalysts excellent activity and stability for DRM at atmospheric pressure.

#### REFERENCES

- [1] Wang, S.B., Lu, G.Q. 2000. Effects of promoters on catalytic activity and carbon deposition of Ni/gamma-Al<sub>2</sub>O<sub>3</sub> catalysts in CO<sub>2</sub> reforming of CH<sub>4</sub>. *Journal of Chemical Technology and Biotechnology*, 75 (7), 589-595.
- [2] Subramani, V., Gangwal, S.K. 2008. A review of recent literature to search for an efficient catalytic process for the conversion of syngas to ethanol. *Journal of Energy & Fuels*, 22 (2), 814-839.

[3] Levy, B. 1973. Platinum-Like Behavior of Tungsten Carbide in Surface Catalysis. *Science*, 181.

[4] De Novion, C.H., Landesman, J. 1985. Order and disorder in transition metal carbides and nitrides: experimental and theoretical aspects. *Pure and Applied Chemistry*, 57 (10), 1391-1402.

[5] Yang, H., Xu, Z., Fan, M. 2008. Progress in carbon dioxide separation and capture: A review. *Journal of Environmental Sciences*, 20 (1), 14-27.

[6] Huang, J., Ma, R., Huang, T. 2011. Carbon dioxide reforming of methane over Ni/Mo/SBA-15-La<sub>2</sub>O<sub>3</sub> catalyst: Its characterization and catalytic performance. *Journal of Natural Gas Chemistry*, 20 (5), 465-470.

[7] Shi, C., Zhang, A., Li, X. 2012. Ni-modified Mo<sub>2</sub>C catalysts for methane dry reforming. *Applied Catalysis A: General*, 431, 164-170.

[8] Zhang, A., Zhu, A., Chen, B. 2011. In-situ synthesis of nickel modified molybdenum carbide catalyst for dry reforming of methane. *Catalysis Communications*, 12 (9), 803-807.

[9] Zhang, Y., Zhang, S., Zhang, X. 2015. Ni Modified WC<sub>x</sub> Catalysts for Methane Dry Reforming[M]//*Advances in CO<sub>2</sub> Capture, Sequestration, and Conversion*. *Journal of American Chemical Society*, 171-189.

[10] Shi, C., Zhang, S., Li, X. 2014. Synergism in NiMoO<sub>x</sub> precursors essential for CH<sub>4</sub>/CO<sub>2</sub> dry reforming. *Catalysis Today*, 233, 46-52.

